# Self-Aggregation Tendency of All Species Involved in the Catalytic Cycle of Bifunctional Transfer Hydrogenation

| | |
|---|---|
| Journal: | *Organometallics* |
| Manuscript ID: | om-2008-009552 |
| Manuscript Type: | Article |
| Date Submitted by the Author: | 03-Oct-2008 |
| Complete List of Authors: | Macchioni, Alceo; University of Perugia, Chemistry<br>Ciancaleoni, Gianluca; University of Perugia, Department of Chemistry<br>Zuccaccia, Cristiano; University of Perugia, Department of Chemistry<br>Zuccaccia, Daniele; University of Perugia, Department of Chemistry<br>Clot, Eric; Université de Montpellier 2, Institut Charles Gerhardt |
| | |

# Self-Aggregation Tendency of All Species Involved in the Catalytic Cycle of Bifunctional Transfer Hydrogenation

*Gianluca Ciancaleoni,*[a] *Cristiano Zuccaccia,*[a] *Daniele Zuccaccia,*[a]

*Eric Clot,*[b*] *and Alceo Macchioni*[a*]

[a]Dipartimento di Chimica, Università di Perugia, via Elce di Sotto, 8, 06123 Perugia (Italy)

[b]Institut Charles Gerhardt (UMR 5253 CNRS-UM2-ENSCM-UM1), Equipe CTMM, Case Courrier 1501, Université de Montpellier 2, 34095 Montpellier Cedex 5 (France)

**Abstract**. The self-aggregation tendency of [RuX(N,N)($\eta^6$-*p*-cymene)] [N,N = amino amidate, X = Cl (**1**) and H (**2**)] and [Ru(N,N)($\eta^6$-*p*-cymene)] [N,N = amido amidate, **3**] in various solvents was investigated by diffusion NMR spectroscopy. The proper evaluation of the molecular hydrodynamic volume of the **1**-**3** monomeric species allowed understanding that **1** and **2** are mainly present as monomers in isopropanol-$d_8$ at concentrations below the millimolar level. Dimers start to become relevant at concentrations over ca. 10 mM [$\Delta G^0$(aggregation) = - 2.2 kcal mol$^{-1}$]. The self-aggregation tendency of **1**-**2** in $CDCl_3$ is marked [$\Delta G^0$(aggregation) = - 3.4 kcal mol$^{-1}$] and much higher than that of

* To whom correspondence should be addressed. Email: alceo@unipg.it; Fax: +39 075 5855598; Phone: +39 075 5855579

**3**. In toluene-$d_8$, **3** and **1** readily form dimers and higher aggregates, respectively, even at millimolar concentrations. The structures and energetics of **1**-**1**, **2**-**2**, and **3**-**3** dimers were investigated by ONIOM (B3PW91/HF) calculations. It was found that the main interaction at the origin of the dimerization process is the establishment of an intermolecular H-bond between one N-H on one monomer and the oxygen of the $SO_2$ moiety of the other. In **3**, the amido group is less acidic and less spatially available for H-bonding than in **1** and **2**, which explains the reduced tendency to form dimers.

## Introduction

Weak interactions occurring in the second coordination sphere of organometallic complexes may profoundly alter their reactivity.[1] The formation of supramolecular adducts held together by non-covalent intermolecular interactions in solution can be directly evaluated by detecting intermolecular dipolar interactions between the constituting units in the NOE-based NMR experiments[2] or, indirectly, by measuring the average hydrodynamic size of supramolecular adducts through diffusion NMR spectroscopy.[3] The selection of proper peripheral functional groups and solvents has allowed clear evidence to be obtained regarding the formation of non-covalent aggregates higher than ion pairs and dimers,[4] such as ion quadruples,[5] cationic ion triples,[6] dications[7] and extended aggregates, even of nanometric dimension.[8] Nevertheless, an experimentally-supported rationale of the effects of intermolecular interactions on the chemical reactivity of organometallics, based on intermolecular structural modifications, has rarely been found.[9]

Asymmetric transfer hydrogenation of ketones and imines is a key reaction in fine chemicals and pharmaceutical synthesis and many studies have been carried out to design and develop chiral catalysts.[10] Noyori and coworkers led to a breakthrough in this field when they discovered some ruthenium-based catalysts, bearing the BINAP[11] and DPEN[12] ligands, capable of reducing ketones *via* transfer hydrogenation with very high enantioselectivity.

The novelty of the Ru-DPEN system stems from its bifunctional catalytic mechanism that, based on detailed investigations,[13,14] occurs without direct substrate/metal interaction. The three important species of the catalytic cycle are reported in Scheme 1. **1** is the precatalyst;[12] **2** is the hydride complex that donates both $H^-$ and $H^+$ to the substrate that is to be transfer-hydrogenated (bifunctional mechanism); and **3** is the 16-electron bis-amido species that regenerates **2** upon reaction with a hydrogen donor (usually isopropanol or HCOOH). Weak second-coordination-sphere interactions (hydrogen bonds, CH/π interactions) are essential for controlling the relative catalyst/substrate orientation which determines the efficiency and stereoselectivity of the transfer hydrogenation. It should be noted that, all the species in Scheme 1 bear an electro-negative moiety (the sulfonyl group) and an electropositive one (the protic NH moiety), that are suitable for establishing inter-molecular hydrogen bonds that can lead to their self-aggregation in solution, analogously to what is observed for the Shvo's catalyst.[15]

In a preliminarily communication[16] we reported the marked tendency of precatalyst **1** (Scheme 1) to self-aggregate in many solvents. As a follow-up to that work, we report, in full, the self-aggregation tendency of **1**, of the hydride **2**, in chloroform, isopropanol, and toluene, and of the 16-electron diamido species **3**, in chloroform, toluene and methylene chloride.

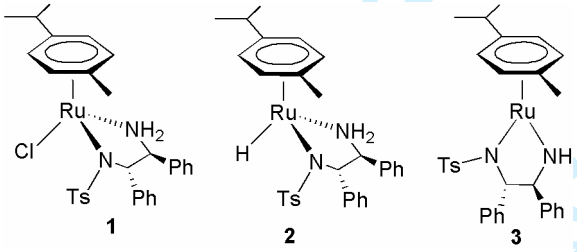


**Scheme 1**

In order to disclose the level of self-aggregation under conditions as similar as possible to those used in catalysis, the salt and temperature effects on the self-aggregation were investigated. Furthermore, ONIOM(B3PW91/HF) calculations were performed on the monomers (**1**, **2**, and **3**) and on the dimers (**1-1**, **2-2**, and **3-3**), in an attempt to clarify the self-aggregation process.

## Results and Discussion

**PGSE NMR Measurements**. A systematic diffusional study was carried out for complexes **1**, **2**, and **3** in order to evaluate their self-aggregation tendency. Experimental data are listed in Table 1. $D_t$ values were evaluated by means of the PGSE (Pulsed-field Gradient Spin Echo) NMR technique and related to molecular sizes through the modified Stokes-Einstein equation (Eq. 1):[17]

$$D_t = \frac{kT}{f_s c \pi \eta r_H} \quad (1)$$

where k is the Boltzmann constant, T is the temperature, $f_s$ is the shape factor, c is a numerical factor, η is the solution viscosity and $r_H$ is the hydrodynamic radius. $V_H^{sph}$ was calculated assuming a spherical shape ($f_s$ = 1) for both the monomer and the aggregates (Table 1). $N_{vdW}$ is defined as the ratio $V_H^{sph}/V_{vdW}$, the latter being calculated from X-Ray data[12b] of **1**, **2**, and **3** (459, 435 and 430 Å$^3$, respectively). $V_H^{pro}$ and $N_{pro}$ were calculated assuming that the monomer and aggregates have spherical and prolate ellipsoid ($f_s > 1$, see below) shapes, respectively.

**Table 1**. Diffusion coefficient ($10^{10}D_t$, $m^2s^{-1}$), average hydrodynamic volume in the spherical ($V_H^{sph}$, Å$^3$) and ellipsoidal ($V_H^{pro}$, Å$^3$) approximations, aggregation numbers ($N_{vdW}$, $N_{pro}$) and concentration (C, mM), for compounds **1**, **2** and **3** in different solvents.

| Entry | Solvent | $10^{10}$ $D_t$ | $V_H^{sph}$ | $N_{vdW}$ | $V_H^{pro}$ | $N_{pro}$ | C |
|---|---|---|---|---|---|---|---|
| | | | **1** | | | | |
| 1 | $CDCl_3$ | 6.08 | 1087 | 2.4 | 1073 | 1.3 | 2.0 [a] |
| 2 | $CDCl_3$ | 4.65 | 2242 | 4.9 | 1982 | 2.4 | 12 [a] |
| 3 | $CDCl_3$ | 3.61 | 4126 | 9.0 | 2890 | 3.5 | 29 |
| 4 | toluene-$d_8$ | 2.64 | 9634 | 21.0 | 4683 | 5.7 | 20 |
| 5 | toluene-$d_8$ | 3.02 | 6488 | 14.1 | 3747 | 4.5 | 4.0 |
| 6 | 2-propanol-$d_8$ | 1.70 | 833 | 1.8 | 826 | 1.0 | 0.05[a] |
| 7 | 2-propanol-$d_8$ | 1.69 | 842 | 1.8 | 834 | 1.0 | 0.2 [a] |
| 8 | 2-propanol-$d_8$ | 1.60 | 988 | 2.2 | 966 | 1.2 | 1.0 [a] |
| 9 | 2-propanol-$d_8$ | 1.55 | 1051 | 2.3 | 1040 | 1.3 | 4.0 [a] |
| 10 | 2-propanol-$d_8$ | 1.37 | 1264 | 2.8 | 1238 | 1.5 | 12 [a] |

| | | | | | | | | |
|---|---|---|---|---|---|---|---|---|
| | 11 | 2-propanol-$d_8$ | 1.15 | 1823 | 4.0 | 1651 | 2.0 | 42 [a] |
| | | | | **2** | | | | |
| 12 | | $CDCl_3$ | 6.72 | 1129 | 2.6 | 1092 | 1.4 | 2.4 |
| 13 | | $CDCl_3$ | 4.85 | 2369 | 5.4 | 1950 | 2.5 | 12.6 |
| 14 | | $CDCl_3$ | 4.77 | 2625 | 6.0 | 2106 | 2.7 | 15.6 |
| 15 | | $CDCl_3$ | 2.88 | 7458 | 17.1 | 3899 | 5.0 | 57.0 |
| 16 | | 2-propanol-$d_8$ | 1.90 | 873 | 2.0 | 858 | 1.1 | 0.47 |
| 17 | | 2-propanol-$d_8$ | 1.86 | 923 | 2.1 | 916 | 1.2 | 1.1 |
| 18 | | 2-propanol-$d_8$ | 1.79 | 1008 | 2.3 | 991 | 1.3 | 7.4 |
| | | | | **3** | | | | |
| 19 | | $CDCl_3$ | 7.59 | 755 | 1.8 | 747 | 1.3 | 1.1 |
| 20 | | $CDCl_3$ | 7.49 | 826 | 1.9 | 816 | 1.4 | 4.4 |
| 21 | | $CDCl_3$ | 6.66 | 909 | 2.1 | 878 | 1.5 | 52 |
| 22 | | toluene-$d_8$ | 6.37 | 800 | 1.4 | 759 | 1.3 | 4.0 |
| 23 | | toluene-$d_8$ | 4.73 | 1282 | 2.3 | 822 | 1.9 | 25 |
| 24 | | $CD_2Cl_2$ | 10.2 | 589 | 1.4 | 589 | 1.0 | 1.0 |
| 25 | | $CD_2Cl_2$ | 9.92 | 648 | 1.5 | 630 | 1.1 | 8.0 |

[a] From ref. 16.

It can be seen that for all the complexes, $V_H^{sph}$ is always much higher than $V_{vdW}$, even at low concentration values (Table 1). This does not necessarily mean that complex **1** is significantly present as a dimer at the lowest investigated concentration;[16] it could be due to the deviation of the hydrodynamic volume ($V_H^0$) of the single molecule from $V_{vdW}$.[5e,18] For this reason, we decided to carefully evaluate $V_H^0$s.

**Evaluation of $V_H^0$.** The correct evaluation of the hydrodynamic volume of the aggregating units ($V_H^0$) is essential for quantitatively investigating any associative process. Nevertheless, it is difficult to predeict $V_H^0$ because it can subtly deviate from van der Waals and crystallographic volumes.[17] One way to evaluate $V_H^0$ is to perform diffusion NMR experiments under conditions where aggregation in solution is negligible (extremely diluted conditions). Unfortunately, such experiments are very time-consuming. A simple and rapid methodology for evaluating $V_H^0$ of ionic species that takes advantage of the complementarities of PGSE and conductometric NMR measurements has recently been proposed.[18] In fact, the formation constant of ion-pairs ($K_{IP}$) can be easily measured by means of conductivity studies, while the average volumes of cations and anions can be obtained from a single diffusional NMR

measurement. If the latter is conducted under conditions where only free ions and ion pairs are present in solution, $V_H^{+0}$ and $V_H^{-0}$ can be straightforwardly obtained.[18] Furthermore, if the hydrodynamic volume of the anion is known, it is even possible to obtain $V_H^{+0}$ and the dissociation degree from a single PGSE measurement performed under the above-mentioned conditions.[18] In order to apply such a methodology for determining $V_H^0$, we selected an ionic compound that is as similar as possible to **1** and **2**. The choice fell on complex **4**$BPh_4$ (Scheme 2) since it can be prepared easily (Experimental Section) and has a counterion whose $V_H^{0-}$ is known.[5e,18]

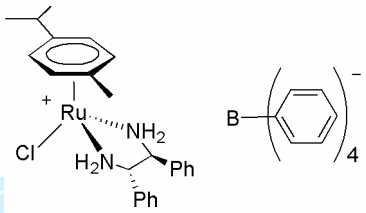


**4**$BPh_4$

**Scheme 2**

PGSE measurements were carried out on **4**$BPh_4$ in $CD_2Cl_2$, in order to measure $V_H^{+0}$(**4**$^+$); the experimental results are shown in Table 2. The $V_{vdW}$(**4**$^+$) value, calculated from the X-Ray structure of **4**Cl,[19] is 353 Å$^3$. The average $V_H^{+0}$ value of 630 Å$^3$, was obtained from diffusion measurements imposing $V_H^{-0}$ = 461 Å$^3$.[18] This value is about 1.8 times higher than that of $V_{vdW}$. The small variations observed for $V_H^{+0}$ with respect to the concentration are within the experimental error, which is ca. 10-15% on $V_H$.

**Table 2**. Diffusion coefficients ($10^{10}D_t$, $m^2s^{-1}$), average hydrodynamic volumes ($V_H$, Å$^3$), concentrations (C, mM), calculated cationic volume ($V_H^{+0}$, Å$^3$), calculated dissociation degree ($\alpha$) and the ratio $V_H^{+0}/V_{vdW}^+$ for **4**$BPh_4$ in $CD_2Cl_2$. $V_H^{-0}$ = 461 Å$^3$ was imposed.[18]

| $D_t^+$ | $D_t^-$ | $V_H^+$ | $V_H^-$ | C | $V_H^{+0}$ | $\alpha$ | $V_H^0/V_{vdW}$ |
|---|---|---|---|---|---|---|---|

| | | | | | | | | |
|---|---|---|---|---|---|---|---|---|
| | 8.80 | 9.04 | 896 | 830 | 0.2 | 621 | 0.41 | 1.76 |
| 8.38 | 8.48 | 1023 | 993 | 2.5 | 639 | 0.17 | 1.80 | |

The high value of the $V_H^{+0}/V_{vdW}^{+}$ ratio for **4**$^+$ can probably be explained by looking at the conformation N,N-ligand (Figure 1). There are two parallel phenyl substituents that generate an inlet containing some "trapped volume"; this is not counted in $V_{vdW}$, but it could be relevant for $V_H^{+0}$. Although **4**$^+$ is not exactly isostructural to **1** and **2**, they have the same ligand conformation, as can be seen by comparing their X-Ray solid-state structures[12b,19] (Figure 1). **4**$^+$ differs from **1** and **2** in that it does not possess the tosylate moiety, but this is probably irrelevant since it does not create any inlet. As a confirmation, ruthenium complexes bearing ($Me_2N$-$CH_2CH_2$-$NMe_2$) and [Ph-N=C(Me)C(Me)=N-Ph] ligands have the same $V_H^{+0}/V_{vdW}^{+}$ ratio, that is about 1.35.[18] So the $V_H^{0}/V_{vdW}$ ratio for **1** and **2** is assumed to be 1.8. In contrast, the two phenyls of the N,N- ligand in **3** are so tightly twisted, that they do not create any inlet. For this compound, $V_H^{0}/V_{vdW}$ should assume the same value as those for other Ru-cymene compounds. In agreement, at the lowest concentration $V_H$ is just 1.4 times $V_{vdW}$ (entry 24, Table 1).

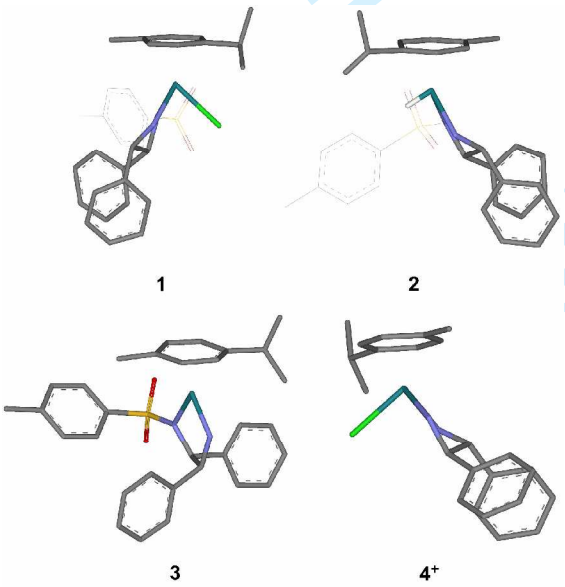


**Figure 1.** Schematic representation of the crystal structure of **1**, **2**, **3** (ref. 12b) and **4**$^+$ (ref. 19).

**Structure of higher aggregates.** Having established $V_H^{0}$, the aggregation level can be determined from the ratio $V_H^{sph}/V_H^{0}$. The spherical approximation (sph) implies that all the aggregates

(monomers, dimers, etc…) are sphere-like. While this approximation seems reasonable for the monomer, it may not be reasonable for the dimer and higher aggregates. To quantitatively estimate the importance of the shape factor ($f_s$), the structure of the aggregates must be hypothesized. From the solid state stuctures[12b] and theoretical calculations (see below) it can be concluded that self-aggregation is driven by HBs between the aminic proton and the sulfonyl group, while the chlorine atom is not involved. Since the interacting functionalities are on opposite sides of the molecule, linear aggregates can be assumed. If a monomer binds to a dimer, it can interact through its oxygen atoms or its aminic protons, but the shape of the resulting trimer will always be linear. The same happens for higher aggregates. Indeed linear aggregates (rows) held together by HBs are present in the solid state[12b] (Figure 2). Furthermore, no specific interaction between rows seems to be present.

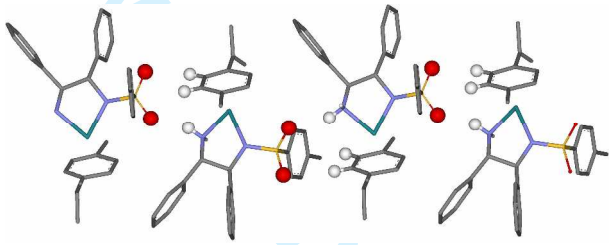

**Figure 2**. A linear non-covalent "tetramer" of **2** as found in the solid-state structure (Ref. 12b).

Linear aggregates can be treated as prolate ellipsoids.[20] Eq. 1 is still valid, but $r_H$ is now defined as the geometric mean of the two semiaxes of the ellipsoid, $\sqrt[3]{a^2b}$ (a is the minor axis, b is the major one for a prolate ellipsoid).

In order to evaluate $f_s$ (see Experimental section) one axis must be known; we have assumed that the minor axis is equal to the hydrodynamic radius of the monomer, $r_H^0$ (5.82 Å for **1**, 5.71 Å for **2**, 5.20 Å for **3**). In fact the "height" of the aggregate remains constant and only its "length" varies with the addition of monomers. In this way if all the factors in Eq. 1 are expressed as a function of a, b and $r_H^{solvent}$, the only unknown parameter is b. The resulting equation can be graphically solved (Experimental Section). $N_{pro}$ can now be defined as $V_H^{pro}/V_H^0$ or $2b/2r_H^0$, that is, the length of the polymer over the diameter of the monomer.

The results are listed in Table 1 and the trends of $N_{pro}$ as a function of the concentration are reported in Figure 3. It is interesting to note that a drastic decrease in the aggregation numbers occurs when the correct $V_H^0$ and shape of the aggregates are taken into account ($N_{pro} << N_{vdW}$).

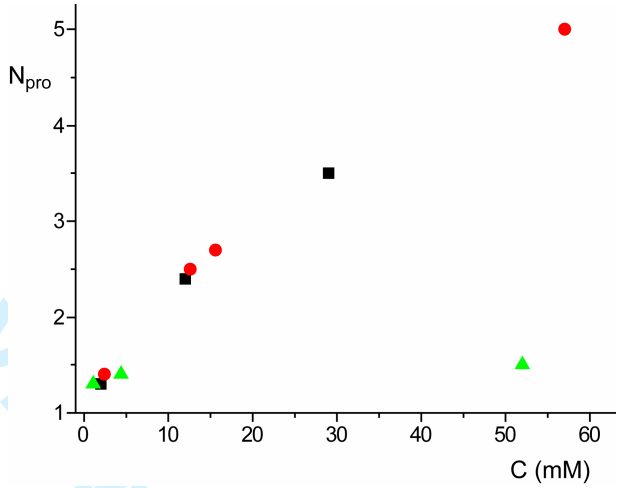


**Figure 3**. Dependence of hydrodynamic volume ($N_{pro}$) on concentration for complexes **1** (■), **2** (●) and **3** (▲) in $CDCl_3$.

Not surprisingly, the $N_{pro}$ values in $CDCl_3$ for complex **2** show the exact same trend as those of **1** (Figure 3), reaching a maximum value of 5.0 (C = 57 mM). On the contrary, **3** exhibits a very low disposition to self-aggregation; in fact, $N_{pro}$ = 1.6 when C = 52 mM (entry 20, Table 1). The tendency of **3** to form non-covalent dimers in $CD_2Cl_2$, which has a greater $\varepsilon_r$ (8.89 instead of 4.81), is still smaller and monomers are prevalently present in solution up to a concentration of 8mM (Table 1, entries 24-25).

Regarding 2-propanol-$d_8$, a certain tendency to form aggregates is present for **1**, but the higher $\varepsilon_r$ value (19.92) strongly depresses it: at C = 12 mM, $N_{pro}$ is 2.4 in chloroform and 1.5 in 2-propanol. As in $CDCl_3$ the self-aggregation of **2** is the same as that of **1** within the experimental error. Obviously, it was not possible to study **3** in this solvent, because the compound reacts immediately with the alcohol to give the hydride **2**.

In toluene-$d_8$, **1** affords aggregates with an average hydrodynamic volume that is 4.5 times higher than that of the monomer already when C = 2 mM (Table 1, entry 5). Although to a lesser degree, **3** self-aggregates in toluene-$d_8$ leading to a significant presence of dimers when C = 25 mM (Table 1, entry

23). These results could be relevant since the amido complex **3** was successfully applied in the asymmetric catalysis of the Micheal reaction[21] carried out in toluene using a catalyst concentration of ca. 20 mM. Our results indicate that under such conditions, dimers and higher aggregates are surely present in solution for complex **3** and for the Ru(DPEN)(cymene)malonate intermediate isolated by Ikariya and co-workers, respectively.[21a] In the soli state, the latter, bearing the $-NH_2$ moiety, exhibits non-covalent rows of H-bonded Ru-units[21a] similar to those found for **1** and **2**. Since the chlorine of **1** is not involved in inter-molecular bonds, it is reasonable to believe that Ru-malonate complex has a self-aggregation tendency similar to **1**.

Transfer hydrogenation reactions are very often carried out at high temperature in the presence of a base, using the chloride complex as precatalyst.[22] Consequently, some PGSE measurements were carried out for **1** at low concentration, higher temperatures[23] and adding KCl[24] in order to mimic catalytic conditions. The results are listed in Table 3. The effect of increasing the temperature on the self-aggregation is difficult to predict because it causes an increase in the thermal agitation, which tends to destroy non-covalent aggregates, but also a reduction of the relative permittivity ($\varepsilon_r$) of the solvent, which strengthens electrostatic interactions and enhances self-aggregation.[25] The data reported in Table 3 clearly show that neither the presence of a salt nor an increased T caused significant variations in the self-aggregation tendency.

**Table 3.** Temperature (T, K), diffusion coefficient ($10^{10}D_t$, $m^2s^{-1}$), average hydrodynamic radius ($r_H$, Å) average hydrodynamic volume ($V_H$, $Å^3$), aggregation number (N), for compound **1** in 2-propanol-$d_8$. [**1**] is always 1 mM.

| Entry | T | $D_t$ | $r_H$ | $V_H$ | N |
|---|---|---|---|---|---|
| 1 | 296 | 1.60 | 6.20 | 988 | 1.2 [a] |
| 2 | 307 | 4.11 | 6.25 | 927 | 1.1 |
| 3 | 321 | 6.18 | 6.30 | 1037 | 1.3 |
| 4 | 328 | 9.04 | 5.93 | 873 | 1.0 |
| 5 | 307 | 3.96 | 6.20 | 984 | 1.2[b] |
| 6 | 321 | 6.42 | 5.90 | 843 | 1.0 [b] |
| 7 | 328 | 4.65 | 6.00 | 905 | 1.1[b] |

[a] From ref. 16 [b] In presence of an excess of KCl.

**Evaluation of the aggregation equilibrium constant**. Since the formation of the non-covalent polymer is driven by the same interaction at every step, the "Equal K (EK) model" can be used to treat the experimental data.[8b,26] EK model assumes that when a monomer is added to the pre-arranged polymer the free energy and equilibrium constant, K, are identical to those corresponding to the addition of previous monomers. Under this assumption, the values of N are related to K through Equation 2: [8b,17]

$$N(N-1) = KC \quad (2)$$

where C is the formal concentration.

Figure 4 shows the trend of $N_{pro}(N_{pro}-1)$ versus the concentration of both **1** and **2** in $CDCl_3$. Since the N *versus* C trends of **1** and **2** are the same, they are considered as a single data set. The fit is very good ($r^2 > 0.99$) and the calculated K is 350 $M^{-1}$. The related variation of free energy $\Delta G^0$ (-3.4 kcal $mol^{-1}$) is consistent with the energy of a hydrogen bond in chloroform.[8b,27]

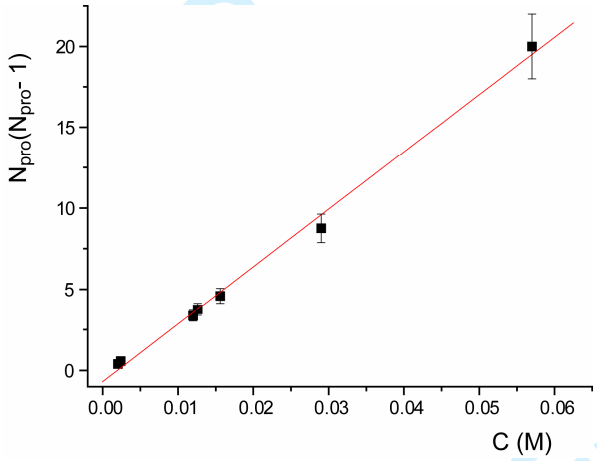


**Figure 4**. Dependence of $N_{pro}(N_{pro}-1)$ on the concentration for **1** and **2** in $CDCl_3$. The Fit equation is $N_{pro}(N_{pro}-1) = -0.7(2)+350(10)C$, $r^2=0.995$.

This result seems to indicate that the main NH···OS interaction is only slightly strengthened by the CH···OS interaction. The same model was applied to the data in 2-propanol: the calculated K is 46 $M^{-1}$ and the related variation of free energy $\Delta G^0$ is -2.2 kcal $mol^{-1}$. This means that at the catalytic concentration (0.05 mM), the room-temperature concentration of **1**-**1** and **2**-**2** dimers is negligible and is equal to 0.2% of the monomer concentration.

**Computational studies.** The experimental studies have shown that compounds **1-3** do self-aggregate in various solvents and that the aggregation tendencies of **1** and **2** are similar and greater than that of **3**. To shed more light on this dimerization process and, in particular, on the structure and energetics of the dimers, ONIOM(B3PW91/HF) calculations were performed on the monomers (**1**, **2**, and **3**) and on the dimers (**1-1**, **2-2**, and **3-3**). Due to the size of the systems, a hybrid ONIOM strategy was employed. The substituents of the cymene ring (Me and $^{i}$Pr), the phenyl and tolyl groups of the N-N ligand have been described at the HF/DZ level, while the rest of the molecule has been treated at the B3PW91/DZP level (see Computational Details).

Table 4 shows a comparison between the experimental and calculated values for a series of selected geometrical parameters. There is an excellent agreement and the ONIOM(B3PW91/HF) methodology adopted allows for the description of these systems. In particular, the orientation of the cymene ring, with respect to the N-N ligand, is faithfully reproduced (within 2° for **1** and **3**, and within 8° for **2**). The larger value (ca. 70°) observed for the δ value in **3** is due to the absence of the "extra" ligand in **1** (Cl) and **2** (H), thus alleviating steric repulsions. The substituents of the cymene ring now occupy the empty space.

**Table 4.** Comparison of selected geometrical parameters (distances in Å, angles in degrees) for the compounds **1**, **2**, and **3**. $N_a$ is the nitrogen atom bearing H atoms, while $N_b$ is the nitrogen atom connected to $SO_2$; $C_a$ is the carbon atom on the cymene ring bearing the methyl substituent; D is the centroid of the six aromatic carbon of the cymene ring; δ is the torsional angle $C_a$-D-Ru-$N_b$.

| | **1** | | **2** | | **3** | |
|---|---|---|---|---|---|---|
| | Exp. | Calc. | Exp. | Calc. | Exp. | Calc. |
| Ru-Cl | 2.435 | 2.425 | | | | |
| Ru-H | | | 1.452 | 1.580 | | |
| Ru-$N_a$ | 2.116 | 2.119 | 2.108 | 2.120 | 1.897 | 1.905 |
| Ru-$N_b$ | 2.145 | 2.139 | 2.139 | 2.151 | 2.065 | 2.078 |
| Ru-D | 1.669 | 1.666 | 1.677 | 1.708 | 1.673 | 1.660 |
| $N_a$-Ru-$N_b$ | 79.5 | 78.6 | 78.3 | 77.8 | 78.9 | 79.5 |
| δ | 37.0 | 37.7 | 33.6 | 25.6 | 71.7 | 69.2 |

There are obviously many different ways to bring two monomers together to form a dimer. However, a full search of the configuration space would be extremely costly in terms of computational resources. In the present case, the driving force for the dimerization is expected to be a H-bond developing between a N-H bond on the N-N ligand of one monomer and an oxygen atom of the $SO_2$ group of the other monomer. The piano stool geometry of the complex has been shown to give inverted geometries in the higher order aggregates.[28] Therefore, the guesses regarding the geometries for the optimization procedure of the dimer were built introducing the two characteristics mentioned above: the NH···O H-bond, and an inverted geometry for the piano stool. Figure 5 shows the structures of the dimers obtained at the ONIOM(B3PW91/HF) level and Table 5 reports selected geometrical parameters and formation energy, $\Delta_{dim}E$. The latter values were estimated through single point B3PW91/DZP calculations on the ONIOM(B3PW91/HF) optimized geometries (see Computational Details).

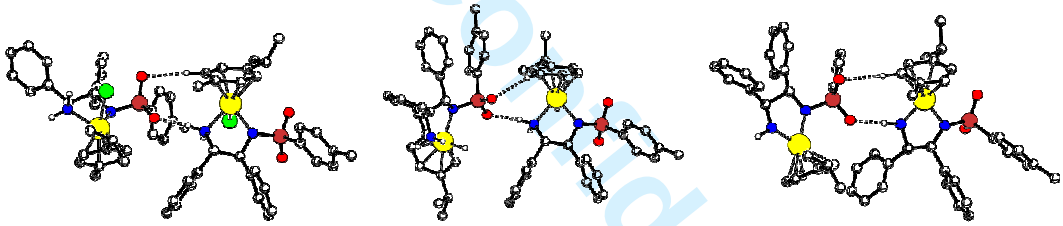


**Figure 5**. ONIOM(B3PW91/HF) optimized geometries for the dimers **1-1**, **2-2**, and **3-3** of the three systems studied. All of the hydrogen atoms except the ones involved in the H-bonding network and on the nitrogen atom have been omitted for clarity.

**Table 5.** Selected geometrical parameters (distances in Å) for the H-bond network present in the dimers **1-1**, **2-2**, **3-3**. $\delta_a$ is the torsional angle (degrees, see Table 4 for definition) for the cymene ring that is not involved in the H-bond network, while $\delta_b$ is the torsion angle for the cymene ring involved in the H-bond network. Formation energy (kcal $mol^{-1}$) of the dimer, $\Delta_{dim}E$.

| | 1-1 | 2-2 | 3-3 |
|---|---|---|---|
| N-H…O | 1.942 | 2.048 | 2.124 |
| C-H…O | 2.492 | 2.855 | 2.591 |
| $\delta_a$ | 40.6 | 20.8 | 73.7 |
| $\delta_b$ | 88.2 | 45.3 | 116.7 |
| $\Delta_{dim}E$ | -10.3 | -9.2 | -8.4 |

The main interaction at the origin of the dimerization process is the creation of a H-bond between one N-H bond on one monomer and an oxygen atom of the $SO_2$ group of the other. The strength of this H-bond, as estimated from the value of the NH…O contact (Table 5), correlates with the formation energy $\Delta_{dim}E$. The second oxygen atom of the $SO_2$ group is involved in a weaker H-bond with a C-H bond ortho to the Me group on cymene. The length of the CH…O contact does not follow the trends observed in $\Delta_{dim}E$. However, the creation of the H-bond is sufficiently stabilizing that it induces a torsion of the cymene ring as indicated by the values of the torsional angles, $\delta_b$, with respect to the $\delta$ values for the monomers (Tables 4 and 5). The cymene ring rotates by ca. 30-40° with respect to the orientation in the monomer. For the other cymene ring, that is not involved in the H-bond network, the $\delta_a$ value of the torsional angle in the dimer (Table 5) is very close to that of the $\delta$ in the monomer (Table 4).

Experimentally the Gibbs free energy of the formation of the dimer depends on the nature of the solvent; the values are ca. -2 to -3 kcal $mol^{-1}$ for **1-1** and **2-2**, whereas no value could be obtained for **3-3**. It is not easy to calculate the entropy contributions in condensed phase and the calculations in gas phase usually overestimate the translational component of the entropy contribution.[29] The latter is generally thought to contribute the majority of the 8 to 10 kcal $mol^{-1}$ loss in the Gibbs free energy upon formation of an AB complex between two molecules of A and B.[30]

Qualitatively, the loss of Gibbs free energy in the dimerization process is estimated to be ca. 8 kcal $mol^{-1}$. This would lead to slightly negative values for $\Delta_{dim}G°$ for **1** and **2**, and thermoneutral value for **3**

(Table 5). These results are in qualitative agreement with the experimental observations. The aggregation of the monomer is essentially driven by the creation of a H-bond between N-H on one monomer and $SO_2$ on the other. Changing to a solvent that is more prone to be engaged in H-bonding interactions could hamper the dimerization process as observed experimentally. As the $NH_2$ group of **1** and **2** have similar acidities, the aggregation tendencies for these two compounds are found to be similar. For **3**, the amido NH group is less acidic and less spatially available for H-bonding. The 16-electron nature of **3** has modified the overall geometry at Ru and the NH bond is buried more deeply within the complex. The H-bond is not strong enough to compensate for the loss of entropy in the dimerization process.

## Conclusions

A systematic $^1$H PGSE NMR study was carried out for all the species involved in the catalytic cycle of bifunctional transfer hydrogenation. It was found that the precatalyst **1** and the hydride complex **2** have the same self-aggregation tendencies that are much higher than that of the 16-electron complex **3**. ONIOM calculations on dimer formations clearly showed that **3** has less tendency to self-aggregate due to the lower acidity and less spatial availability of the amido NH group.

In 2-propanol-$d_8$, **1** and **2** are prevalently present as monomers up to a concentration of ca. 10 mM. In contrast, complexes **1**-**3** readily form dimers and larger aggregates even at millimolar concentrations in $CDCl_3$ and toluene-$d_8$. Increasing the temperature and/or adding KCl has little effect on the self aggregation tendency of **1** in 2-propanol-$d_8$.

It can be concluded that from a thermodynamic point of view, dimers are not very relevant for transfer hydrogenation carried out in 2-propanol, while they must be taken into consideration when catalytic reactions are carried out in low polar solvents.

## Experimental Section

All reagents were purchased from Sigma-Aldrich or Ricci Chimica and used without any further purification. Compounds **1**-**4** were synthesized according to the literature,[12b] using the standard Schlenk technique. Solvents, deuterated and not, were freshly distilled (n-hexane with Na, $Et_2O$ with Na/benzophenone, 2-propanol with $CaH_2$, methylene chloride and chloroform with $P_2O_5$) and degassed, by many gas-pump-nitrogen cycles before use. All Van der Waals volumes was computed from the crystal structures using the WebLab ViewerLite 4.0 software packages.

**Synthesis of $4BPh_4$.** A solution of (*S*,*S*)-1,2-diphenyl-ethylendiamine (60 mg, 0.283 mmol) and $[Ru(\eta^6\text{-}p\text{-cymene})Cl_2]_2$ (86.6 mg, 0.142 mmol) in methylene chloride was stirred for 2 hours. Then, $NaBPh_4$ (97 mg, 0.283 mmol) was added and, immediately, a white solid (NaCl) precipitated. The solution was filtered off and n-hexane was added to obtain the desired product (181.6 mg, 80%), that was washed with n-hexane, diethyl ether and dried under reduced pressure. The product was crystallized from a methylene chloride/methanol/diethyl ether solution. $^1$H NMR ($CD_2Cl_2$, 298 K); 7.40 (br, 8H, *o*-Ph, anion), 7.34 (m, 3H, Ph, cation), 7.31 (m, 3H, Ph, cation), 7.05 (m, 12H, Ph, cation and anion), 6.93 (t, 4H, $J_{HH}$ = 6.9 Hz, *p*-Ph, anion), 5.27 (d, 1H, $J_{HH}$ = 6.1 Hz, cymene), 5.23 (d, 1H, $J_{HH}$ = 6.2 Hz, cymene), 5.11 (d, 1H, $J_{HH}$ = 6.1 Hz, cymene), 5.01 (d, 1H, $J_{HH}$ = 6.2 Hz, cymene), 3.88 (m, 1H, C*H*Ph), 3.66 (m, 1H, C*H*Ph), 2.70 (sept, 1H, $J_{HH}$ = 7.1 Hz, C*H*$(CH_3)_2$), 2.11 (s, 3H, $CH_3$), 1.22 (m, 6H, CH(C*H*$_3)_2$). Anal. Calcd. for $C_{48}H_{50}BN_2Ru$: C, 75.18; H, 6.57; N, 3.65. Found: C, 74.95; H, 7.03; N, 3.50.

**PGSE NMR Measurements**.[31] $^1$H NMR measurements were performed by using the standard stimulated echo pulse sequence[31] on a Bruker AVANCE DRX 400 spectrometer equipped with a GREAT 1/10 gradient unit and a QNP probe with a Z-gradient coil, at 296 K without spinning. All the measurements at high temperature were performed by using the double stimulated echo pulse sequence, with LED implemented.[32]

The dependence of the resonance intensity (I) on a constant waiting time and on a varied gradient strength (G) is described by Equation 3:

$$\ln\frac{I}{I_0} = -(\gamma\delta)^2 D_t\left(\Delta - \frac{\delta}{3}\right)G^2 \quad (3)$$

where I = intensity of the observed spin echo, $I_0$ = intensity of the spin echo without gradients, $D_t$ = diffusion coefficient, Δ = delay between the midpoints of the gradients, δ = length of the gradient pulse, and γ = magnetogyric ratio. The shape of the gradients was rectangular, their duration (δ) was 4-5 ms, and their strength (G) was varied during the experiments. All of the spectra were acquired using 32K points, a spectral width of 5000 ($^1$H) Hz, and processed with a line broadening of 1.0 ($^1$H) Hz. After having checked that a change in total relaxation time (from 5 to 130 s) did not affect the measurement results, standard experiments were carried out with a total recycle time of 5 s. The semilogarithmic plots of $\ln(I/I_0)$ versus $G^2$ were fitted using a standard linear regression algorithm; the *R* factor was always higher than 0.99. Different values of Δ, "nt" (number of transients), and number of different gradient strengths were used for different samples.

The self-diffusion coefficient $D_t$, that is directly proportional to the slope of the regression line obtained by plotting $\log(I/I_0)$ *vs.* $G^2$ (equation 3), was estimated by measuring the proportionality constant as previously described.[17,33] The uncertainty in the measurements was estimated by determining the standard deviation of the slopes of the linear regression lines by performing experiments with different Δ values. The standard propagation of error analysis gave a standard deviation of approximately 3-4% in hydrodynamic radii and 10-15% in hydrodynamic volumes and aggregation numbers N.

**Treatment of $D_t$ data**. $D_t$ were evaluated for compounds (sa) and TMSS (st, the internal standard) as described before. From Eq. 4 the ratio of the $D_t$ values for TMSS and compounds, equal to the ratio of the slopes (m) of the straight lines coming from plotting $\log(I/I_0)$ vs $G^2$, is

$$\frac{m^{sa}}{m^{st}} = \frac{D_t^{sa}}{D_t^{st}} = \frac{c^{st} r_H^{st}}{f_s^{sa} c^{sa} (\sqrt[3]{a^2 b})^{sa}} = f(r_{solv}, r_H^{st}, a, b) \quad (4)$$

The latter circumvents the dependence of the $D_t$ values on temperature, solution viscosity, and gradient calibration. TMSS has the shape of a sphere, then $f_s^{st} = 1$ and a = b. While $c^{st} r_H^{st}$ is known from previous

measurements,[33b] $f_s^{sa}c^{sa}(\sqrt[3]{a^2b})^{sa}$ can be evaluated from Eq. 5, since the $m^{sa}/m^{st}$ ratio was measured, and expressed as a function of $r_{solv}$, a and b as:

$$f_s^{sa}c^{sa}(\sqrt[3]{a^2b})^{sa} = \frac{\sqrt{1-\frac{a^2}{b}}}{\sqrt[3]{\frac{a^2}{b}}\times \ln\left(\frac{1+\sqrt{1-\frac{a^2}{b}}}{\frac{a}{b}}\right)} \times \frac{6}{\left[1+0.695\left(\frac{r_{solv}}{\sqrt[3]{a^2b}}\right)^{2.234}\right]} \times \sqrt[3]{a^2b} \qquad (5)$$

Since a is fixed from chemical hypothesis, the only unknown parameter is b. The complicated Eq. 5 can be solved graphically.

**Computational Details.** All the calculations have been performed with the Gaussian03 package.[34] ONIOM(B3PW91/HF) calculations[35] were performed, where the methyl and isopropyl groups on the cymene ligand, the phenyl and tolyl groups on the N-N ligand were treated at the HF level. The rest of the systems was treated at the DFT level with the hybrid functional B3PW91.[36] For the DFT part of the calculations the ruthenium atom was represented by the relativistic effective core potential (RECP) from the Stuttgart group and the associated basis set,[37] augmented by an f polarization function.[38] The Cl and S atoms were represented by RECP from the Stuttgart group and the associated basis set,[39] augmented by a d polarization.[40] The remaining atoms (C, H, N, O) were represented by a 6-31G(d,p) basis set.[41] For the lower level in the ONIOM calculations treated at the HF level, the Ru, Cl, and S atoms were treated with the Los Alamos RECP and the associated basis set,[42] while the remaining atoms were treated with a 4-31G basis set.[43] Full optimization of geometry without any constraint were performed followed by analytical computation of the Hessian matrix to confirm the nature of the located extrema as minima on the potential energy surface. The formation energies, $\Delta_{dim}E$, of the dimers were evaluated by single point calculations at the B3PW91 level with the basis set described above for both the monomer and the dimer in the ONIOM optimized geometry.

**Acknowledgment**. We thank the Ministero dell'Università e della Ricerca (MUR, Rome, Italy), COST, CNRS (E.C.) and the Dow Chemical Company for support.

**Supporting Information Available**. Procedure to evaluate $V_H^{0+}$ from diffusion data. Plots of $Ln(I/I_0)$ versus $G^2$. This material is available free of charge via the Internet at http://pubs.acs.org.

## References

(1) (a) Das, S.; Brudvig, G. W.; Crabtree, R. H. *Chem. Commun.* **2008**, 413. (b) Das, S.; Brudvig, G. W.; Crabtree, R. H. *J. Am. Chem. Soc.* **2008**, *130*, 1628. (c) Machut, C.; Patrigeon, J.; Tilloy, S.; Bricout, H.; Hapiot, F.; Monflier, E. *Angew. Chem. Int. Ed.* **2007**, *46*, 3040. (d) Leung, D. H.; Bergman, R. G.; Raymond, K. N. *J. Am. Chem. Soc.* **2007**, *129*, 2746. (e) Das, S.; Incarvito, C. D.; Crabtree, R. H.; Brudvig, G. W. *Science* **2006**, *312*, 1941. (f) Krämer, R. *Angew. Chem. Int. Ed.* **2006**, *45*, 858. (g) Roelfes, G.; Feringa, B. L. *Angew. Chem. Int. Ed.* **2005**, *44*, 3230. (h) Thomas, C. M.; Ward, T. R. *Chem. Soc. Rev.* **2005**, *34*, 337. (i) Macchioni, A. *Chem. Rev.* **2005**, *105*, 2039.

(2) Macchioni, A. *Eur. J. Inorg. Chem.* **2003**, 195 and references therein.

(3) (a) Binotti, B.; Macchioni, A.; Zuccaccia, C.; Zuccaccia, D. *Comments Inorg. Chem.* **2002**, *23*, 417. (b) Pregosin, P. S.; Martinez-Viviente, E.; Kumar, P. G. A. *Dalton Trans.* **2003**, 4007. (c) Pregosin, P. S.; Kumar, P. G. A.; Fernández, I. *Chem. Rev.* **2005**, *105*, 2977. (d) Pregosin, P. S. *Prog. Nucl. Magn. Reson. Spectrosc.* **2006**, *49*, 261.

(4) Bellachioma, G.; Ciancaleoni, G.; Zuccaccia, C.; Zuccaccia, D.; Macchioni, A. *Coord. Chem. Rev.* **2008**, *252*, 2224.

(5) (a) Beck, S.; Geyer, A.; Brintzinger, H.-H. *Chem. Commun.* **1999**, 2477. (b) Zuccaccia, C.; Stahl, N. G.; Macchioni, A.; Chen, M.-C.; Roberts, J. A.; Marks, T. J. *J. Am. Chem. Soc.* **2004**, *126*, 1448. (c)

Song, F.; Lancaster, S. J.; Cannon, R. D.; Schormann, M.; Humphrey, S. M.; Zuccaccia, C.; Macchioni, A.; Bochmann, M. *Organometallics* **2005**, *24*, 1315. (d) Alonso-Moreno, C.; Lancaster, S. J.; Zuccaccia, C.; Macchioni, A.; Bochmann, M. *J. Am. Chem. Soc.* **2007**, *129*, 9282. (e) Zuccaccia, D.; Bellachioma, G.; Cardaci, G.; Ciancaleoni, G.; Zuccaccia, C.; Clot, E.; Macchioni, A. *Organometallics* **2007**, *26*, 3930.

(6) Zuccaccia, D.; Foresti, E.; Pettirossi, S.; Sabatino, P.; Zuccaccia, C.; Macchioni, A. *Organometallics* **2007**, *26*, 6099.

(7) Bolaño, S.; Ciancaleoni, G.; Bravo, J.; Gonsalvi, L.; Macchioni, A.; Peruzzini, M. *Organometallics* **2008**, *27*, 1649.

(8) (a) Macchioni, A.; Romani, A.; Zuccaccia, C.; Guglielmetti, G.; Querci, C. *Organometallics* **2003**, *22*, 1526. (b) Ciancaleoni, G.; Di Maio I.; Zuccaccia, D.; Macchioni, A. *Organometallics* **2007**, *26*, 489. (c) Rocchigiani, L.; Zuccaccia, C.; Zuccaccia, D.; Macchioni, A. *Chem. Eur. J.* **2008**, *14*, 6589.

(9) Binotti, B.; Bellachioma, G.; Cardaci, G.; Carfagna, C.; Zuccaccia, C.; Macchioni, A. *Chem. Eur. J.* **2007**, *13*, 1570.

(10) (a) Noyori, R.; Hashiguchi, S. *Acc. Chem. Res.* **1997**, *30*, 97; (b) Palmer, M. J.; Willis, M. *Tetrahedron: Asymmetry* **1999**, *10*, 2045; (c) Everaere, K.; Mortreux, A.; Carpentier, J.-F. *Adv. Synth. Catal.* **2003,** *345*, 67; (d) Clapham, S. E.; Hadzovic, A.; Morris, R. H. *Coord. Chem. Rev.* **2004**, *248*, 2201; (d) Gladiali, S.; Alberico, E. *Chem. Soc. Rev.* **2006**, *35*, 226; (e) Ikariya, T.; Blacker, J. *Acc. Chem. Res.* **2007**, *40*, 1300.

(11) (a) Miyashita, A.; Yasuda, A.; Takaya, H.; Toriumi, K.; Ito, T.; Souchi, T.; Noyori, R. *J. Am. Chem. Soc.* **1980,** *102*, 7932; (b) Miyashita, A.; Takaya, H.; Souchi, T.; Noyori, R. *Tetrahedron* **1984**, *40*, 1245; (c) Noyori, R.; Takaya, H. *Acc. Chem. Res.* **1990**, *23*, 345.

(12) (a) Hashiguchi, S.; Fujii, A.; Takehara, J.; Ikariya, T.; Noyori, R. *J. Am. Chem. Soc.* **1995,** *117*, 7562; (b) Haack, K. J.; Hashiguchi, S.; Fukii, A.; Ikariya, T.; Noyori, R. *Angew. Chem. Int. Ed. Engl.* **1997**, *36*, 285; for the synthesis of the ligand see (c) Oda, T.; Irie, R.; Katsuki, T.; Okawa, H. *Synlett* **1992**, 641.

(13) (a) Noyori, R.; Ohkuma, T. *Angew. Chem. Int. Ed. Engl.* **2001**, *40*, 40; (b) Noyori, R. *Angew. Chem., Int. Ed.* **2002**, *41*, 2008; (c) Noyori, R.; Yamakawa, M.; Hashiguchi, S. *J. Org. Chem.* **2001**, *66*, 7931.

(14) Samec, J. S. M.; Bäckvall, J. E.; Andersson, P. G.; Brandt, P. *Chem. Soc. Rev.* **2006**, *35*, 237.

(15) Casey, C. P.; Johnson, J.B.; Singer, S. W.; Cui, Q. *J. Am. Soc. Chem.* **2005**, *127*, 3100.

(16) Zuccaccia, D.; Clot, E.; Macchioni, A. *New J. Chem.* **2005**, *29*, 430.

(17) Macchioni, A.; Ciancaleoni, G.; Zuccaccia, C.; Zuccaccia, D. *Chem. Soc. Rev.* **2008**, *37*, 479.

(18) Ciancaleoni, G.; Zuccaccia, C.; Zuccaccia, D.; Macchioni, A. *Organometallics* **2007**, *26*, 3624.

(19) Jones, M. D.; Almeida Paz, F. A.; Davies, J. E.; Raja, R.; Klinowski, J.; Johnson, B. F. G. *Inorg. Chim. Acta* **2004**, *357*, 1247.

(20) Allouche, L.; Marquis, A.; Lehn, J. M. *Chem. Eur. J.* **2006**, *12*, 7520.

(21) (a) Watanabe, M.; Murata, K.; Ikariya T. *J. Am. Chem. Soc.* **2003**, *125*, 7508; (b) Watanabe, M.; Ikagawa, A.; Wang, H.; Murata, K.; Ikariya T. *J. Am. Chem. Soc.* **2004**, *126*, 11148.

(22) Ru: KOH: Substrate = 1: 5: 200, with [Substrate] = 0.1 M, T = 80°C, in 2-propanol, see rif. 12a.

(23) For a recent reference on temperature effect see: Giordani, C.; Wakai, C.; Okamura, E.; Matubayasi, N.; Nakahara, M. J. *Phys. Chem. B* **2006**, *110*, 15205.

(24) For some recent references on salt effect see: (a) Di Biasio, A.; Bordi, F.; Cametti, C. *Prog. Colloid Polym. Sci.*, **2004**, *123*, 78-82; (b) Zhu, A.; Dai, S.; Li, L.; Zhao, F. *Colloids Surf., B*, **2006**, *47*, 20; (c) Slavnova, T. D.; Chibisov, A. K.; Görner, H. *J. Phys Chem. A*, **2005**, *109*, 4758; (d) Mallamace, F.; Scolaro, L. M.; Romeo, A.; Micali, N. *Phys. Rev. Lett.*, **1999**, *82*, 3480; (e) Laus, S.; Sitharaman, B.; Tóth, É.; Bolskar, R. D.; Helm, L.; Asokan, S.; Wong, M. S.; Wilson, L. J.; Merbach, A. E. *J. Am. Chem. Soc.*, **2005**, *112*, 9368.

(25) The reduction of $\varepsilon_r$ with the increasing of temperature in alcohol is more marked than in aprotic solvents. This is because the high value of $\varepsilon_r$ depends not only from the polarization of the single molecule, but arises from the cooperative properties of the solvent and the presence of a network of hydrogen bonds. For example passing from 280 to 300 K, $\varepsilon_r$ (chloroform) diminishes of about 11%, $\varepsilon_r$ (acetone) of 15% and $\varepsilon_r$ (2-propanol) of 22% (data from CRC Handbook of Chemistry and Physics, 85$^{th}$ edition, **2003**, New York).

(26) (a) Ts'O, P. O. P.; Melvin, I. S.; Olson, A. C. *J. Am. Chem. Soc.* **1963**, *85*, 1289. (b) Martin, R. B. *Chem. Rev.* **1996**, *96*, 3043, and references therein.

(27) (a) Rivas, J. C. M.; Salvagni, E.; de Rosales, R. T. M. *Dalton Trans.* **2003**, *17*, 3339; (b) Yajima, T.; Maccarrone, G.; Takani, M.; Contino, A.; Arena, G.; Takamido, R.; Hanaki, M.; Funahashi, Y.; Odani, A.; Yamauchi, O. *Chem. Eur. J.* **2003**, *9*, 3341.

(28) (a) Brunner, H. *Angew. Chem., Int. Ed.* **1999**, *38*, 1194. (b) Brunner, H. *Eur. J. Inorg. Chem.* **2001**, 905.

(29) Cooper, J.; Ziegler, T. *Inorg. Chem.* **2002**, *41*, 6614.

(30) Watson, L.; Eisenstein, O. *J. Chem. Ed.* **2002**, *79*, 1269.

(31) Valentini, M.; Rüegger, H.; Pregosin, P.S. *Helv. Chim. Acta* **2001**, *84*, 2833 and references therein.

(32) (a) Jerschow, A.; Mueller, N. *J. Magn. Reson. A* **1996**, *123*, 222. (b) Jerschow, A.; Mueller, N. *J. Magn. Reson. A* **1997**, *125*, 372.

(33) Zuccaccia, D.; Macchioni, A. *Organometallics* **2005**, *24*, 3476.

(34) Gaussian 03, Revision C.02, Frisch, M. J.; Trucks, G. W.; Schlegel, H. B.; Scuseria, G. E.; Robb, M. A.; Cheeseman, J. R.; Montgomery, Jr., J. A.; Vreven, T.; Kudin, K. N.; Burant, J. C.; Millam, J. M.; Iyengar, S. S.; Tomasi, J.; Barone, V.; Mennucci, B.; Cossi, M.; Scalmani, G.; Rega, N.; Petersson, G. A.; Nakatsuji, H.; Hada, M.; Ehara, M.; Toyota, K.; Fukuda, R.; Hasegawa, J.; Ishida, M.; Nakajima, T.; Honda, Y.; Kitao, O.; Nakai, H.; Klene, M.; Li, X.; Knox, J. E.; Hratchian, H. P.; Cross, J. B.; Bakken, V.; Adamo, C.; Jaramillo, J.; Gomperts, R.; Stratmann, R. E.; Yazyev, O.; Austin, A. J.; Cammi, R.; Pomelli, C.; Ochterski, J. W.; Ayala, P. Y.; Morokuma, K.; Voth, G. A.; Salvador, P.; Dannenberg, J. J.; Zakrzewski, V. G.; Dapprich, S.; Daniels, A. D.; Strain, M. C.; Farkas, O.; Malick, D. K.; Rabuck, A. D.; Raghavachari, K.; Foresman, J. B.; Ortiz, J. V.; Cui, Q.; Baboul, A. G.; Clifford, S.; Cioslowski, J.; Stefanov, B. B.; Liu, G.; Liashenko, A.; Piskorz, P.; Komaromi, I.; Martin, R. L.; Fox, D. J.; Keith, T.; Al-Laham, M. A.; Peng, C. Y.; Nanayakkara, A.; Challacombe, M.; Gill, P. M. W.; Johnson, B.; Chen, W.; Wong, M. W.; Gonzalez, C.; and Pople, J. A.; Gaussian, Inc., Wallingford CT, 2004.

(35) Svensson, M. ; Humbel, S. ; Froese, R. D. J. ; Matsubara, T. ; Sieber, S. ; Morokuma, K. *J. Phys. Chem.* **1996**, *100*, 19357.

(36) (a) Becke, A. D. *J. Chem. Phys.* **1993**, *98*, 5648. (b) Perdew, J. P.; Wang, Y. *Phys. Rev. B* **1992**, *45*, 13244.

(37) Andrae, D.; Haussermann, U.; Dolg, M.; Stoll, H.; Preuss, H. *Theor. Chim. Acta* **1990**, *77*, 123.

(38) Ehlers, A. W.; Bohme, M.; Dapprich, S.; Gobbi, A.; Hollwarth, A.; Jonas, V.; Kohler, K. F.;Stegmann, R.; Veldkamp, A.; Frenking, G. *Chem. Phys. Lett.* **1993**, *208*, 111.

(39) Bergner, A.; Dolg, M.; Kuchle, W.; Stoll, H.; Preuss, H. *Mol. Phys.* **1993**, *80*, 1431.

(40) Hollwarth, A.; Bohme, M.; Dapprich, S.; Ehlers, A. W.; Gobbi, A.; Jonas, V.; Kohler, K. F.; Stegmann, R.; Veldkamp, A.; Frenking, G. *Chem. Phys. Lett.* **1993**, *208*, 237.

(41) Hariharan, P. C.; Pople, J. A. *Theor. Chim. Acta* **1973**, *28*, 213.

(42) (a) Wadt, W. R. ; Hay, P. J. *J. Chem. Phys.* **1985**, *82*, 284. (b) Hay, P. J. ; Wadt, W. R. *J. Chem. Phys.* **1985**, *82*, 299.

(43) R. Ditchfield, R. ; Hehre, W. J. ; Pople, J. A. *J. Chem. Phys.* **1971**, *54*, 724.

- FOR TABLE OF CONTENTS USE ONLY -

# Self-Aggregation Tendency of All Species Involved in the Catalytic Cycle of Bifunctional Transfer Hydrogenation

*Gianluca Ciancaleoni,*[a] *Cristiano Zuccaccia,*[a] *Daniele Zuccaccia,*[a]

*Eric Clot,*[b*] *and Alceo Macchioni*[a*]

[a]Dipartimento di Chimica, Università di Perugia, via Elce di Sotto, 8, 06123 Perugia (Italy)

[b]Institut Charles Gerhardt (UMR 5253 CNRS-UM2-ENSCM-UM1), Equipe CTMM, Case Courrier 1501, Université de Montpellier 2, 34095 Montpellier Cedex 5 (France)

**Abstract**. The self-aggregation tendency of [RuX(N,N)($\eta^6$-*p*-cymene)] [N,N = amino amidate, X = Cl (**1**) and H (**2**)] and [Ru(N,N)($\eta^6$-*p*-cymene)] [N,N = amido amidate, **3**] in solution was investigated by diffusion NMR spectroscopy; **2** and **3** are mainly present as monomers in 2-propanol-$d_8$ below millimolar concentration levels. In $CDCl_3$ and toluene-$d_8$, **1**-**3** readily form dimers even at millimolar concentrations.

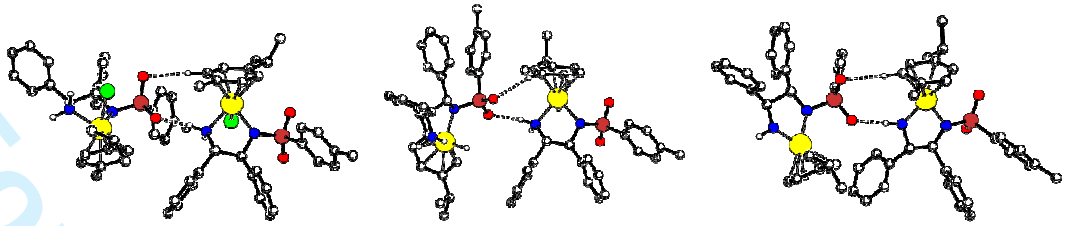

1-1 2-2 3-3